Data Centers as Dispatchable Loads to Harness Stranded Power

Kibaek Kim, *Member, IEEE*, Fan Yang, *Member, IEEE*, Victor M. Zavala, *Member, IEEE*, and Andrew A. Chien, *Fellow, IEEE*

Abstract—We analyze how traditional data center placement and optimal placement of dispatchable data centers affect power grid efficiency. We use detailed network models, stochastic optimization formulations, and diverse renewable generation scenarios to perform our analysis. Our results reveal that significant spillage and stranded power will persist in power grids as wind power levels are increased. A counter-intuitive finding is that collocating data centers with inflexible loads next to wind farms has limited impacts on renewable portfolio standard (RPS) goals because it provides limited system-level flexibility. Such an approach can, in fact, increase stranded power and fossil-fueled generation. In contrast, optimally placing data centers that are dispatchable provides system-wide flexibility, reduces stranded power, and improves efficiency. In short, optimally placed dispatchable computing loads can enable better scaling to high RPS. In our case study, we find that these dispatchable computing loads are powered to 60–80% of their requested capacity, indicating that there are significant economic incentives provided by stranded power.

Index Terms—Cloud computing, energy markets, green computing, power grid, renewable portfolio standard (RPS), renewable power.

I. INTRODUCTION

OVER the past two decades, a growing consensus on climate change due to anthropogenic carbon [1], [2] has emerged. In response, efforts have expanded worldwide to reduce the amount of carbon being released into the atmosphere [3], [4]. Information and computing technologies (ICT) emissions, estimated at 2% in 2010 of global emissions [5], are among the most rapidly growing. In fact, recent estimates put ICT emissions at 8% of electric power in 2016, growing to 13% by 2027 [5], [6]. The rise of cloud computing has led to growing concerns about carbon emissions from data centers [6], spawning research on data-center energy efficiency [7], [8] and

how to exploit renewable power [9]–[12]. A recent strategy pursued by several "hyperscaler" internet companies is to purchase wind-power offsets as part of "long-term purchase" contracts [13]. Another well-studied research topic is the optimization of data-center site selection based on cost and on exploitation of renewable power [14], [15]. To the best of our knowledge, all such studies consider costs and benefits from a cloud computing operator perspective, seeking to maximize individual data center revenue, reduce total cost of ownership (TCO), and maintain high data-center availability. In this paper, we consider the impact of the addition of new data centers and collocated renewables on *system-level* resilience, efficiency, and flexibility of the power grid.

Closely related work includes study of data-center demand-response (DCDR) [16] and how to implement it in data centers by affecting scheduling and providing economic incentives to data center tenants [17], [18]. These models employ grid economic incentives and aim to reduce data center load by $15 \sim 20\%$ on demand. A fundamental challenge for such approaches is that data-center operators are not inclined to participate - even with significant pricing incentives, because power cost is typically $<10\%$ of data-center TCO, and demand-response involves adding significant operational complexity. In contrast, we consider a new model where the data center is treated by ISOs as a "dispatchable load," based on new computer science approaches to create flexible computing loads [19], [20]. This produces two advantages: (1) much larger dynamic range for load (100% of the data-center use vs. 15%) and (2) elimination of the need to convince traditional data center operators to undertake DCDR.[1]

Ambitious "renewable portfolio standards" (RPS) goals for renewable power as a fraction of overall power have been widely adopted. Midwest examples from the mid-continent independent system operator (MISO) system include Illinois (25% by 2025) to Minnesota ($25 \sim 31\%$ by 2025). California and New York have adopted a 50% goal by 2030 [21], [22]. Obama's "Clean Power Plan," issued August 2015, calls for a national 32% reduction in electric power carbon emissions by 2030, with renewable power as a critical element. And, the U.S. Department of Energy landmark report "Wind Vision 2015" describes how the United States can achieve a 35% RPS for wind alone by 2050, a big jump from a combined solar and wind RPS of 5.2% in 2014 [23]. In this plan, some regions such as the Midwest and Texas achieve RPS over 50% by 2050. These ambitious

---

[1]This framing does not preclude the possibilities that these dispatchable data centers will receive favorable economic treatment from the grid, since they can provide a significant positive benefit.

and transformative goals pose serious power grid challenges, including the ability to achieve merit order, efficiency, stability, and resiliency.

With dual goals of high RPS in the power grid and support for large-scale computing, we address three questions:

1) What is the impact of data centers on the future power grid?
2) Should renewable generators be collocated with data centers?
3) Can we enable growing cloud computing and renewable penetration?

To explore these questions, we developed a computational framework that combines a detailed power grid network models and cutting-edge parallel optimization solvers to identify optimal designs that remain resilient in the face of a wide range of operational scenarios. We consider different settings that are variations of today's Western Electricity Coordinating Council (WECC) grid: a base system, the addition of twenty 200 MW data centers at random locations, the same twenty data centers with collocated renewables and inflexible loads, and the same data centers with dispatchable loads (volatile cloud computing) and optimally placed in the system. Such dispatchable loads can enable grid efficiency at higher RPS levels because they enable system-wide flexibility. We consider optimizing the location of these dispatchable loads and the resulting impact on power grid efficiency. For each case we characterize the impact of increasing RPS levels and data centers on grid system cost, stranded power, stability, and the capacity achieved by the data centers. Our findings include the following.

1) Significant spillage and stranded power exists in current power grids and increases with higher RPS levels.
2) Collocating wind farms and data centers can in fact be harmful to RPS goals, increasing stranded power and thermal generation.
3) Dispatchable computing loads reduce stranded power and enable higher RPS.
4) Optimizing dispatchable load locations decreases system-wide cost and powers the dispatchable data centers to $60 \sim 80\%$ of capacity.

The rest of the paper is organized as follows. In Section II we introduce concepts of stranded power and dispatchable computing loads. Section III outlines the optimization models, followed by experiments in Section IV. In Section V we summarize our results and briefly discuss future work.

II. STRANDED POWER AND DISPATCHABLE COMPUTING

A. Stranded Power

Power system operators must balance power flows across the network. Generators offer their generation capability to the grid in real time (every 5 to 12 min), and the grid dispatches generation based on the demand and transmission. Intrinsic variability of renewable generation (wind, solar, etc.) creates major challenges for power dispatch. Despite best efforts to match generation and demand, in the process of ensuring reliable power, oversupply and transmission congestion can prevent generated
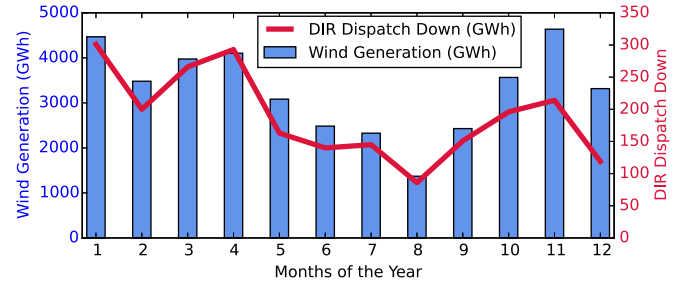

Fig. 1. Wind generation and down-dispatching (spillage) of MISO in 2014.
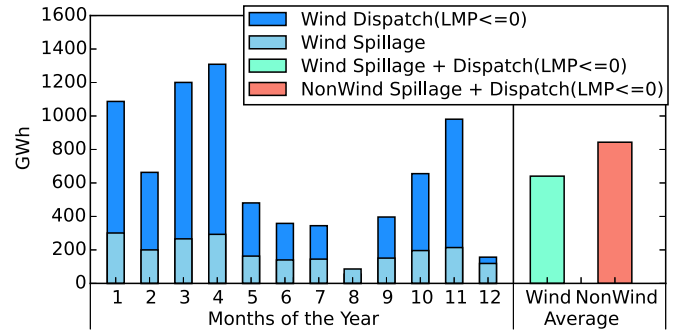

Fig. 2. MISO stranded power (wind) vs. stranded power (nonwind) in 2014.

power from reaching loads at certain times. Power grids call this excess power *spillage*, "curtailment," or "down dispatching."

Fig. 1 shows the monthly wind generation and down-dispatched wind power (spillage) of the MISO system. Almost 7% of wind generation is curtailed because of transmission congestion. The total down-dispatched power of MISO for 2014 was 2.2 terawatt-hours, corresponding to a 183 MW sustained rate. Comparable waste also exists in other independent system operators (ISO), including the Eastern Region Coordinating District of Texas, California ISO (CAISO) [24], and many European countries such as Denmark, Germany, Ireland, and Italy [25]. The amount of waste is projected to increase with higher RPS levels [22].

Modern energy markets dispatch generation by assigning locational marginal prices (LMPs) that vary across generation sites, grid nodes, and time intervals. In situations of oversupply or transmission congestion, power prices can be low or even negative, causing power generators to dump power (spillage) or deliver it and pay the grid to take it.[2] Consequently, spillage can be significantly less than total uneconomic generation.

We define *stranded power* as all offered generation with no economic value, thus including both spillage and delivered power with zero or negative LMP. Fig. 2 presents MISO's stranded power in 2014, breaking it down by month and type. It also compares the average stranded power from wind and nonwind generation. Overall stranded wind power, the sum of wind spillage and noneconomic wind dispatch (LMP ≤ 0), is

---

[2]Delivering power into the grid can be tied to "production tax credits," a financial incentive to sell power to the grid even at negative price.

7.7 TWh for 2014. Interestingly, the nonwind sites, mostly thermal generators, have 10.1 TWh of stranded power. However the thermal generators, experience stranded power as a much lower percentage (8 times lower), because 90% of grid power is thermal.

B. Dispatchable Loads

We define *dispatchable loads* as adjustable (flexible) demands that are dispatched in real time by the power grid. Adjustable at each dispatch time interval, dispatchable loads are an ideal way of demand response and appear promise to reduce congestion and stranded power due to generation variability. Key properties of dispatchable loads include the following.

1) Grid control can increase consumption to limit.
2) Grid control can decrease consumption to zero.
3) Grid control can be exercised at the dispatch interval (instantly).

A less obvious benefit of dispatchable loads is their ability to control network flows (operators currently have limited control over flows as electricity follows paths of least resistance).

We consider one possible type of dispatchable load: computing. Operating on a short time scale, computing has the potential to be agile yet still productive. We call such intermittent computing resources zero-carbon clouds (ZCClouds) and have described and analyzed several possible models [19], [20]. For example, ZCClouds can be computing hardware deployed in shipping containers and directly connected to a wind farm or at a key transmission bottleneck in the power grid. ZCClouds can transform stranded power into computing power with short latency (in seconds) and can be easily turned on or shut down according to stranded power availability. Possible uses include data-center workloads such as big data analysis, machine learning, or high-performance computing. The uptime and capabilities of intermittent computing resources deployed as dispatchable loads are determined by the quantity and temporal distribution of stranded power.

The idea of intermittent (or "volatile") computing resources is of growing interest. Cloud providers have begun to provide unreliable/revokable resources including Amazon's spot instances [26] and Google's preemptible virtual machine Instance [27]. Several studies propose methods to make such resources useful for high-performance computing and more advanced cloud services [28]. We believe there is a broad application for intermittent computing resources.

Many other realizations of dispatchable loads are possible, including energy storage. A key difference, however, is that dispatchable loads have infinite capacity (can run forever without filling up) and avoid subsidized economics (computing services defray their cost by providing services not related to energy).

III. OPTIMIZATION MODELS

In this section we present two optimization models in order to assess the benefits of dispatchable loads. We also present various performance metrics to conduct our analysis.

We begin with the model notation in the following table. The units for power, energy, and phase angles are megawatts, megawatt-hours, and degrees; respectively.

Sets:

$\mathcal{D}; \mathcal{D}_n$	Demand loads; demand loads at bus n
$\mathcal{G}; \mathcal{G}_n$	Generators; generators at bus n
$\mathcal{I}; \mathcal{I}_n$	Import points; import points at bus n
$\mathcal{L}$	Transmission lines
$\mathcal{L}_n^+; \mathcal{L}_n^-$	Transmission lines to bus n; lines from bus n
$\mathcal{N}$	Buses
$\mathcal{R}; \mathcal{R}_n$	Renewable generators; Renewable generators at bus n
$\mathcal{T}$	Time periods
$\mathcal{W}$	Wind-farm locations
Ω	Scenarios

Parameters:

B_l	Susceptance of transmission line l
C_i	Generation cost of generator i
C_j^d	Load-shedding penalty at load j
C_i^w	Spillage penalty at wind farm i
C_i^m	Spillage penalty at import point i
C_i^r	Spillage penalty at renewable i
C_n^s	Value of lost dispatchable load at bus n
D_{jt}	Demand load of consumer j at time t
$F_l^{\max}$	Maximum power flow of transmission line l
K	Maximum number of dispatchable loads
M_{it}	Power production of import i at time t
$P_i^{\max}$	Maximum power output of generator i
R_{it}	Power production of renewable i at time t
RU_i	Ramp-up limit of generator i
RD_i	Ramp-down limit of generator i
U	Dispatchable load capacity
W_{wt}	Power from wind farm w at time t
$W_{wt}(\omega)$	Power from wind farm w at time t for scenario ω
$\pi(\omega)$	Probability of wind production scenario ω
$\Theta_{nt}^{\min}$	Minimum phase angle at bus n at time t
$\Theta_{nt}^{\max}$	Maximum phase angle at bus n at time t

Decision variables:

d_{jt}	Load shedding at load j at time t
$d_{jt}(\omega)$	Load shedding at load j at time t for scenario ω
f_{lt}	Power flow of line l at time t
$f_{lt}(\omega)$	Power flow of line l at time t for scenario ω
m_{it}	Spillage at import i at time t
$m_{it}(\omega)$	Spillage at import i at time t for scenario ω
p_{it}	Power from generator i at time t
$p_{it}(\omega)$	Power from generator i at time t for scenario ω
r_{it}	Spillage at renewable i at time t
$r_{it}(\omega)$	Spillage at renewable i at time t for scenario ω
$u_{nt}(\omega)$	Dispatchable load served at bus n at time t for scenario ω
w_{it}	Spillage at wind farm i at time t
$w_{it}(\omega)$	Spillage at wind farm i at time t for scenario ω
x_n	Number of dispatchable loads installed at bus n
θ_{nt}	Phase angle at bus n at time t
$\theta_{nt}(\omega)$	Phase angle at bus n at time t for scenario ω

A. Economic Dispatch (ED) Model

To assess the economic benefits of dispatchable computing loads, we use the following ED model:

$$\min \quad \sum_{t\in\mathcal{T}} \left(\sum_{i\in\mathcal{G}} C_i p_{\mathrm{it}} + \sum_{j\in\mathcal{D}} C_j^d d_{\mathrm{jt}} + \sum_{i\in\mathcal{I}} C_i^m m_{\mathrm{it}} \right.$$
$$\left. + \sum_{i\in\mathcal{W}} C_i^w w_{\mathrm{it}} + \sum_{i\in\mathcal{R}} C_i^r r_{\mathrm{it}} \right) \quad (1a)$$

$$\text{s.t.} \quad \sum_{l\in\mathcal{L}_n^+} f_{\mathrm{lt}} - \sum_{l\in\mathcal{L}_n^-} f_{\mathrm{lt}} + \sum_{i\in\mathcal{G}_n} p_{\mathrm{it}} + \sum_{i\in\mathcal{I}_n} (M_{\mathrm{it}} - m_{\mathrm{it}})$$
$$+ \sum_{i\in\mathcal{W}_n} (W_{\mathrm{it}} - w_{\mathrm{it}}) + \sum_{i\in\mathcal{R}_n} (R_{\mathrm{it}} - r_{\mathrm{it}})$$
$$= \sum_{j\in\mathcal{D}_n} (D_{\mathrm{jt}} - d_{\mathrm{jt}}), \; (\lambda_{\mathrm{nt}}), \; \forall n\in\mathcal{N}, t\in\mathcal{T}, \quad (1b)$$

$$f_{\mathrm{lt}} = B_l(\theta_{\mathrm{nt}} - \theta_{\mathrm{mt}}), \quad \forall l = (m,n) \in \mathcal{L}, t\in\mathcal{T}, \quad (1c)$$

$$-RD_i \leq p_{\mathrm{it}} - p_{i,t-1} \leq RU_i, \quad \forall i\in\mathcal{G}, t\in\mathcal{T}, \quad (1d)$$

$$-F_l^{\max} \leq f_{\mathrm{lt}} \leq F_l^{\max}, \quad \forall l\in\mathcal{L}, t\in\mathcal{T}, \quad (1e)$$

$$\Theta_n^{\min} \leq \theta_{\mathrm{nt}} \leq \Theta_n^{\max} \quad \forall n\in\mathcal{N}, t\in\mathcal{T}, \quad (1f)$$

$$0 \leq p_{\mathrm{it}} \leq P_i^{\max}, \quad \forall i\in\mathcal{G}, t\in\mathcal{T}, \quad (1g)$$

$$0 \leq d_{\mathrm{jt}} \leq D_{\mathrm{jt}}, \quad \forall j\in\mathcal{D}, t\in\mathcal{T}, \quad (1h)$$

$$0 \leq m_{\mathrm{it}} \leq M_{\mathrm{jt}}, \quad \forall i\in\mathcal{I}, t\in\mathcal{T}, \quad (1i)$$

$$0 \leq w_{\mathrm{it}} \leq W_{\mathrm{jt}}, \quad \forall i\in\mathcal{W}, t\in\mathcal{T}, \quad (1j)$$

$$0 \leq r_{\mathrm{it}} \leq R_{\mathrm{jt}}, \quad \forall i\in\mathcal{R}, t\in\mathcal{T}. \quad (1k)$$

Note that power is supplied from imports, (nonwind) renewables (e.g., bio-, hydro- and geo-) and wind generations as well as from conventional thermal generation units. Considering imports and nonwind renewables (we refer to these simply as renewables in the following discussion) is important because they account for a significant portion of the power generation in some systems. In the CAISO system, for instance, imports and renewables account for 27% and 25% of the total system generation, respectively. Moreover, the analysis that we present later indicates that dispatchable loads can reduce spillage of imports and nonwind renewables. In the presented model we assume that imports as well as renewable and wind power suppliers are not competitive agents in the market (they are high-priority suppliers). Consequently, their supplies are considered as negative demands for which we seek to minimize spillages at costs C_i^m, C_i^w, and C_i^r. We also allow for load shedding at certain nodes at cost C_j^d, which is set to the value of lost load (VOLL).

The objective function (1a) is to minimize the *total dispatch cost*: the sum of supply cost from conventional thermal generators, cost of the load shedding, cost of the import spillage, cost of the wind power spillage, and cost of the nonwind renewable spillage. Note that this objective can be interpreted as maximizing social welfare, as defined in electricity market clearing

models (e.g., [29]). Equation (1b) enforces the power flow balance of the network. Equation (1c) represents a lossless model of power flow equations that determines the power flow of line l by the phase angle difference between two buses m and n. Equation (1d) represents the ramping constraints limiting the rate of change of generation levels. Constraints (1e) and (1f) represent the transmission line capacity and the feasible phase angle range, respectively. Constraint (1g) represents the generation capacity, and constraint (1h) is a bound for the unserved load. Constraints (1i)-(1k) bound spillages of imports, wind, and renewable supply, respectively.

B. Optimal Placement (OP) of Dispatchable Loads

We extend the ED model to account for OP of dispatchable loads at locations minimizing the expected total dispatch cost over multiple wind and load scenarios. This OP model is cast as a two-stage stochastic integer program. Following the convention in the literature (e.g., [30]) we provide the first-stage problem, the second-stage problem, and the deterministic equivalent problem.

1) First-Stage Problem: The first-stage problem is given by

$$\min \quad \mathbb{E}[Q(x,\omega)] \quad (2a)$$

$$\text{s.t.} \quad \sum_{n\in\mathcal{N}} x_n \leq K, \quad (2b)$$

$$x_n \geq 0, \; \text{integer} \quad \forall n\in\mathcal{N}, \quad (2c)$$

where $Q(x,\omega)$ is the recourse function of the first-stage variable x for a given scenario ω. The first-stage decision variable x_n is a here-and-now decision to represent the number and locations of dispatchable loads to be installed at location $n\in\mathcal{N}$. Equation (2b) is a budget constraint for dispatchable loads.

2) Second-Stage Problem: The second-stage problem is given as the recourse function $Q(x,\omega)$ defined for each scenario $\omega\in\Omega$ as follows:

$$\min \sum_{t\in\mathcal{T}} \left(\sum_{i\in\mathcal{G}} C_i p_{\mathrm{it}}(\omega) + \sum_{j\in\mathcal{D}} C_j^d d_{\mathrm{jt}}(\omega) + \sum_{i\in\mathcal{I}} C_i^m m_{\mathrm{it}}(\omega) \right.$$
$$\left. + \sum_{i\in\mathcal{W}} C_i^w w_{\mathrm{it}}(\omega) + \sum_{i\in\mathcal{R}} C_i^r r_{\mathrm{it}}(\omega) \right) \quad (3a)$$

$$\text{s.t.} \; 0 \leq u_{\mathrm{nt}}(\omega) \leq U x_n, \quad \forall n\in\mathcal{N}, t\in\mathcal{T}, \quad (3b)$$

$$\sum_{l\in\mathcal{L}_n^+} f_{\mathrm{lt}}(\omega) - \sum_{l\in\mathcal{L}_n^-} f_{\mathrm{lt}}(\omega) + \sum_{i\in\mathcal{G}_n} p_{\mathrm{it}}(\omega)$$
$$+ \sum_{i\in\mathcal{I}_n} (M_{\mathrm{it}} - m_{\mathrm{it}}(\omega)) + \sum_{i\in\mathcal{W}_n} (W_{\mathrm{it}}(\omega) - w_{\mathrm{it}}(\omega))$$
$$+ \sum_{i\in\mathcal{R}_n} (R_{\mathrm{it}} - r_{\mathrm{it}}(\omega)) - u_{\mathrm{nt}}(\omega)$$
$$= \sum_{j\in\mathcal{D}_n} (D_{\mathrm{jt}} - d_{\mathrm{jt}}(\omega)), \quad \forall n\in\mathcal{N}, t\in\mathcal{T}, \quad (3c)$$

$$f_{\mathrm{lt}}(\omega) = B_l(\theta_{\mathrm{nt}}(\omega) - \theta_{\mathrm{mt}}(\omega)),$$
$$\forall l = (m,n) \in \mathcal{L}, t \in \mathcal{T}, \tag{3d}$$

$$-RD_i \le p_{\mathrm{it}}(\omega) - p_{i,t-1,}(\omega) \le RU_i, \ \forall i \in \mathcal{G}, t \in \mathcal{T}, \tag{3e}$$

$$-F_l^{\max} \le f_{\mathrm{lt}}(\omega) \le F_l^{\max}, \qquad \forall l \in \mathcal{L}, t \in \mathcal{T}, \tag{3f}$$

$$\Theta_n^{\min} \le \theta_{\mathrm{nt}}(\omega) \le \Theta_n^{\max} \qquad \forall n \in \mathcal{N}, t \in \mathcal{T}, \tag{3g}$$

$$0 \le p_{\mathrm{it}}(\omega) \le P_i^{\max}, \qquad \forall i \in \mathcal{G}, t \in \mathcal{T}, \tag{3h}$$

$$0 \le d_{\mathrm{jt}}(\omega) \le D_{\mathrm{jt}}, \qquad \forall j \in \mathcal{D}, t \in \mathcal{T}, \tag{3i}$$

$$0 \le m_{\mathrm{it}}(\omega) \le M_{\mathrm{jt}}, \qquad \forall i \in \mathcal{I}, t \in \mathcal{T}, \tag{3j}$$

$$0 \le w_{\mathrm{it}}(\omega) \le W_{\mathrm{jt}}, \qquad \forall i \in \mathcal{W}, t \in \mathcal{T}, \tag{3k}$$

$$0 \le r_{\mathrm{it}}(\omega) \le R_{\mathrm{jt}}, \qquad \forall i \in \mathcal{R}, t \in \mathcal{T}. \tag{3l}$$

The objective function (3a) is the total dispatch cost with uncertainty arising from wind supply scenarios. The second-stage decisions involve flows, angles, supply, loads, and spillages. Equation (3b) is a capacity constraint for dispatchable loads. The capacity of a dispatchable load is given by U. We note that constraints (3c) include dispatchable loads.

3) Deterministic Equivalent Problem: Assuming that ω has finite support on Ω, the two-stage stochastic programming problem in (2) and (3) can be formulated as a deterministic equivalent problem:

$$\min \sum_{\omega \in \Omega} \pi(\omega) \sum_{t \in \mathcal{T}} \left(\sum_{i \in \mathcal{G}} C_i p_{\mathrm{it}}(\omega) + \sum_{j \in \mathcal{D}} C_j^d d_{\mathrm{jt}}(\omega) \right.$$
$$+ \sum_{i \in \mathcal{I}} C_i^m m_{\mathrm{it}}(\omega) + \sum_{i \in \mathcal{W}} C_i^w w_{\mathrm{it}}(\omega)$$
$$\left. + \sum_{i \in \mathcal{R}} C_i^r r_{\mathrm{it}}(\omega) \right) \tag{4a}$$

$$\text{s.t. } (2b), (2c),$$
$$(3b)\text{-}(3l), \quad \forall \omega \in \Omega. $$

C. Performance Metrics

We define metrics of interest for our analysis. The total amount of power dispatched (absorbed into the system) is given by

$$P_{\mathrm{ED}}^{\mathrm{Dispatch}} := \sum_{t \in \mathcal{T}} \left[\sum_{i \in \mathcal{G}} p_{\mathrm{it}} + \sum_{i \in \mathcal{I}} (M_{\mathrm{it}} - m_{\mathrm{it}}) \right.$$
$$\left. + \sum_{i \in \mathcal{W}} (W_{\mathrm{it}} - w_{\mathrm{it}}) + \sum_{i \in \mathcal{R}} (R_{\mathrm{it}} - r_{\mathrm{it}}) \right]. \tag{5}$$

We differentiate the total power absorbed at positive LMPs and nonpositive LMPs. To do so, we define $\mathcal{N}_t^+ := \{n \in \mathcal{N} : \lambda_{\mathrm{nt}} > 0\}$, where λ_{nt} is an optimal dual variable value of the ED model. The total power absorbed at positive LMPs and nonpositive

TABLE I
AVERAGE LOAD, IMPORTS, RENEWABLE SUPPLY, AND NET LOAD (MW)

	Load	Imports	Renewable	Net Load
SpringWD	26 868	7478	6681	12 708
SpringWE	23 980	7608	6998	9373
SummerWD	31 089	7678	6672	16 737
SummerWE	28 184	7400	7124	13 659
FallWD	28 055	7675	6657	13 722
FallWE	25 186	7108	7065	11 012
WinterWD	26 352	7663	6634	12 054
WinterWE	23 708	6800	5581	11 399

LMPs for ED is given respectively by

$$P_{\mathrm{ED}}^{\mathrm{LMP}>0} := \sum_{t \in \mathcal{T}} \sum_{n \in \mathcal{N}_t^+} \left[\sum_{i \in \mathcal{G}_n} p_{\mathrm{it}} + \sum_{i \in \mathcal{I}_n} (M_{\mathrm{it}} - m_{\mathrm{it}}) \right.$$
$$\left. + \sum_{i \in \mathcal{W}_n} (W_{\mathrm{it}} - w_{\mathrm{it}}) + \sum_{i \in \mathcal{R}_n} (R_{\mathrm{it}} - r_{\mathrm{it}}) \right] \tag{6}$$

and $P_{\mathrm{ED}}^{\mathrm{LMP}\le 0} := P_{\mathrm{ED}}^{\mathrm{Dispatch}} - P_{\mathrm{ED}}^{\mathrm{LMP}>0}$.

We define stranded power as $P_{\mathrm{ED}}^{\mathrm{LMP}\le 0} + P_{\mathrm{ED}}^{\mathrm{Spillage}}$. Wind penetration levels (%) are defined as $100 \times \sum_{i \in \mathcal{W}} \sum_{t \in \mathcal{T}} W_{\mathrm{it}} / \sum_{j \in \mathcal{D}} \sum_{t \in \mathcal{T}} D_{\mathrm{jt}}$. The RPS is defined by the ratio of the renewable power absorbed to the total loads:

$$100 \times \frac{\sum_{t \in \mathcal{T}} \left[\sum_{i \in \mathcal{R}} (R_{\mathrm{it}} - r_{\mathrm{it}}) + \sum_{i \in \mathcal{W}} (W_{\mathrm{it}} - w_{\mathrm{it}}) \right]}{\sum_{j \in \mathcal{D}} \sum_{t \in \mathcal{T}} D_{\mathrm{jt}}}. \tag{7}$$

For the OP model the metrics are defined for each $s \in \mathcal{S}$ from which we compute expected values.

The achieved capacity (%) at time t for a given scenario s is defined as the ratio of the number of data centers served by a positive stranded power: $\sum_{n \in \mathcal{N}} \mathbf{1}(u_{\mathrm{nts}})/K$, where $\mathbf{1}(u_{\mathrm{nts}}) = 1$ if $u_{\mathrm{nts}} > 0$ and zero otherwise.

IV. COMPUTATIONAL RESULTS AND ANALYSES

We study a test system of CAISO interconnected with the WECC. The system consists of 225 buses, 375 transmission lines, 130 generation units, 40 loads, and 5 wind power generation units. We consider a 24-hour horizon with hourly intervals. We use network topology, import supply, renewables, wind production, and load data from [31]. Imports flow into the system through 5 boundary buses. Renewable power is generated from biogas, hydrothermal, and geothermal generators at 11 buses. For this system, the generation capacity that excludes imports, renewables, and wind power is 31.2 GW. We consider load profiles for 8 day types: spring, summer, fall, and winter; and weekday (WD) and weekend (WE). Table I reports average loads, imports, renewables, and net loads (load minus imports, renewables, and wind supply). Fig. 3(a) shows the net loads for the different day types.

For each day type, we use the 1000 specific wind power production scenarios taken from [31] where wind power scenarios are 15% of load, representing the 2020 RPS target of
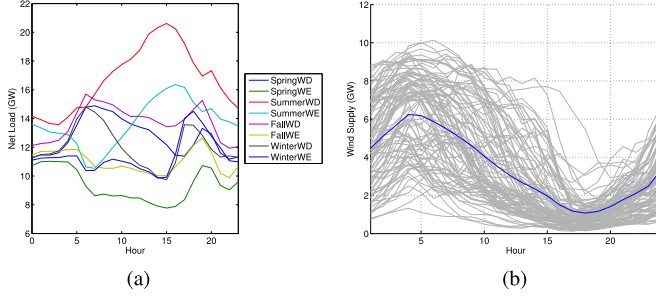
Fig. 3. Net load profile and wind power supply. (a) Net load for each day type. (b) Wind power supply (GW) at 15% level during summer day.

California [31] as illustrated in Fig. 3(b). Each scenario has the same probability $\pi(\omega) = 0.001$ for $\omega \in \Omega$. We chose 1000 scenarios because they are enough for providing the mean objective values with statistical significance p-value < 0.0001 for the four cases. However, the number of sample sizes is not known a priori in general. For readability, we plot only 100 scenarios for wind power (grey lines) to highlight the variability, and we also plot the corresponding mean (blue line). The same wind scenarios are used for WDs and WEs of the same season. We explore a range of additional wind penetration levels: 5%, 15%, 30%, and 50% of load,

As is typical due to longer-term commitments and with the goal of reducing carbon emissions, we assume that imports and renewables are higher priority (i.e., nondispatchable) but can be spilled, if necessary, at a cost of 1000 and 2000 \$ /MWh, respectively. We use a VOLL of 1000 \$ /MWh and a wind spillage cost of 100 \$ /MWh. These values are typical for ISO settings and are chosen to impose a relative priority on different products. The twenty additional 200 MW data centers reflect the rapid growth expected in cloud computing over the next few decades, particularly in the western region. ICT power consumption is estimated at 8% today and projected to grow to as much as $4 \sim 10\%$ per decade [6].

We analyze four cases.

1) Case 1: Base, WECC configuration as described above.
2) Case 2: Case 1 with twenty additional 200 MW data centers that total 4 GW additional load (96 GWh per day). Each data center is a continuous 200 MW load and subject to VOLL penalties. Data-center locations were chosen arbitrarily to reflect choices driven by external business considerations (e.g., networking, proximity to customers, and geographic diversity). The data center loads are inflexible (non-dispatchable).
3) Case 3: Case 2 with collocated wind farms at each data center (with non-dispatchable loads), sized to match total load over 12 months. Because of the typical wind capacity factor of 30%, the peak generation of these farms is typically 3x greater than the 200 MW data-center load.
4) Case 4: Case 1 with twenty additional 200 MW data centers operated as dispatchable loads. The ISO determines the power consumption of each dispatchable load each hour at no penalty cost. The data centers are positioned to minimize overall system dispatch cost across all wind and load scenarios by solving the OP model (2).
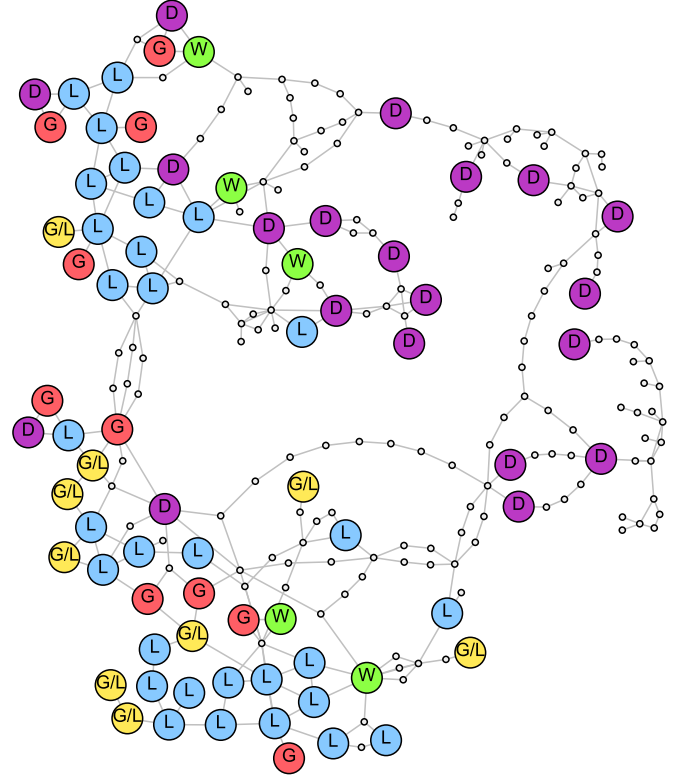

Fig. 4. Node-edge network representation of test system (Cases 2 and 3). The buses with generation units, loads, both generation units and loads, wind units, and data centers are labeled as G, L, G/L, W and D, respectively.

In Cases 1, 2, and 3, we solve the ED model (1), minimizing the total dispatch cost for all wind and load scenarios as we increase wind levels. In Case 4, the ED is subsumed within the OP model, and the solution minimizes the same metrics in addition to OP of dispatchable loads.

The cases vary in total generation and load. We compare percentages relative to Case 1 (i.e., the base system). For example, the loads in Case 2 and 3 are higher because of the addition of data centers with non-dispatchable loads, and Case 4 falls in the middle because of its variable dispatch capacity. We use consistent wind penetration numbers, ignoring the additional wind generation in Case 3. The simple treatment of loads affects "real" wind penetration only $1 \sim 6\%$, far smaller than the resulting spillage. Excluding data-center wind power in Case 3 produces conservative estimates of spillage and stranded power, painting Case 3 in the most favorable light.

Fig. 4 presents a node-edge network representation of the test system with the twenty data center locations of Case 2. We note that this network does not represent the actual geographical locations of the actual buses and the lines of the system. The network was generated by using the `gephi` package [32]. The network system under study is large, and we evaluate a large number of scenarios and system configurations. Thus, the analysis performed is computationally intensive. Cases 1, 2, and 3 solve the ED model (1) for 1000 wind-power scenarios and for each day type and season. These represent a total of 32 008 linear programs (LPs) for each case. Each LP has 19 008 continuous variables and 17 544 linear constraints. Case 4

solves the OP model (2) including all the 1000 wind scenarios; each OP instance is solved for the different day type and season and different wind power levels. We thus solve a total of 24 large-scale stochastic mixed-integer programs (for nonzero wind levels) and 8 deterministic mixed-integer programs (at zero wind level). Each *OP model has 225 general integer variables, 24 408 000 continuous variables, and 22 944 001 constraints.* The ED model was implemented in JuMP [33] and the OP model in StochJuMP [34]. ED is solved with CPLEX 12.6.1, and OP is solved by using the parallel Benders decomposition implementation of the open-source package DSP [35]. DSP is a high-performance optimization package capable of targeting large-scale stochastic programming problems.

All computations were performed on `Blues`, a 310-node computing cluster at Argonne National Laboratory. Each computing node has two octo-core 2.6 GHz Xeon processors and 64 GB of RAM. The computational experiments required the solution of 128 032 LPs, 8 mixed-integer programs, and 24 stochastic mixed-integer programs and post-processing of solution data. In addition to the parallel solver DSP, we used SWIFT [36], a script language for dynamically allocating computing jobs in the parallel cluster. In particular, SWIFT allows us to solve multiple optimization problems in parallel, while each problem is in turn solved in parallel by using DSP. This setting enables us to perform computationally intensive experiments. To give an idea of the efficiency achieved, a single stochastic optimization problem OP was solved in 10 min using 1000 parallel cores (the same problem would have required 166 h if run in a standard serial computer). Running the entire set of computational experiments using DSP and SWIFT required only 25 h of wall-clock time with 2000 computing cores (50 000 core-hours). In contrast, performing such experiments in serial would have required nearly 6 months.

The results reveal important trends that we summarize below. We then present numerical results to illustrate these trends.

1) Case 1 reveals significant spillage and stranded power in the base system due to imports and nonwind renewables. This finding is consistent with the observations of Section II-A. We also observe that, as expected, dispatch cost decreases initially as cheaper wind power displaces thermal generation, but eventually increases because of stranded power penalties. We also see that the variance of the cost increases dramatically as wind level is increased, indicating that the system becomes more vulnerable to wind power variations.

2) Case 2 reveals that positioning large data centers decreases system cost, even if locations are chosen arbitrarily and loads are inflexible. The reason is that the loads put stranded power to work, reducing penalties and moderately reducing system cost. We also observe that while cost is decreased, the variance of the cost is not improved (compared with Case 1).

3) Case 3 reveals that collocating data centers at wind-farm locations gives little benefit to system cost. The slight benefit comes from wind power used to offset the data-center loads, but stranded power is increased as a result of load inflexibility. Case 3 also reveals that collocation
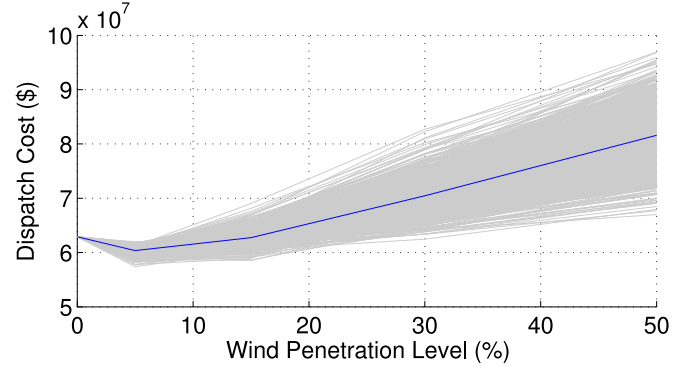

Fig. 5.   Dispatch cost at different wind levels (Case 1).

of data centers and wind farms does not reduce carbon emissions. In fact, it increases thermal generation (and thus emissions) because of increasing stranded power. We found that system cost variance was reduced significantly compared with that of Cases 1 and 2. We attribute this reduction to better utilization of stranded power at data-center locations. This result thus highlights that stranded power can affect system vulnerability.

4) Case 4 reveals that optimally positioned dispatchable loads can reduce power spillage from all sources (imports, nonwind renewables, and wind), not just wind (as in Case 3). Strategic positioning results in decreased system cost and decreased use of thermal generation (and thus emissions). We also find that cost variance is dramatically reduced compared with all other cases, indicating that the system can better manage wind power fluctuations due to increased network flow control. Case 4 also reveals that up to $60 \sim 80\%$ of data center capacity can be achieved at high wind-penetration levels. This result occurs even if loads can be adjusted at no cost. Consequently, data-center owners have a natural economic incentive to provide flexibility. The incentives are provided by better stranded power utilization.

A. Base System

We first analyze the impact of increasing wind levels in Case 1. Fig. 5 shows that the average daily dispatch cost decreases below a 5% wind level, because of the use of cheap wind power. As wind levels increase, however, the dispatch cost is increased by 26% ($ 2.1 MUSD/day) relative to the system at 0% wind level. This increase is a combined effect of using more thermal generation to account for wind power variability and penalties induced by power spillage. Moreover, the system cost becomes more variable as we increase wind levels. In particular, the standard deviation is $ 5.2 MUSD/day at a 50% wind level and $ 0.7 MUSD/day at a 5% wind level. This variability indicates that the system becomes more vulnerable at high wind levels.

Fig. 6(a) shows daily average power and spillage by generation source. As wind penetration is increased form 0% to 50%, thermal generation decreases by 48% (from 349 to 182 GWh).
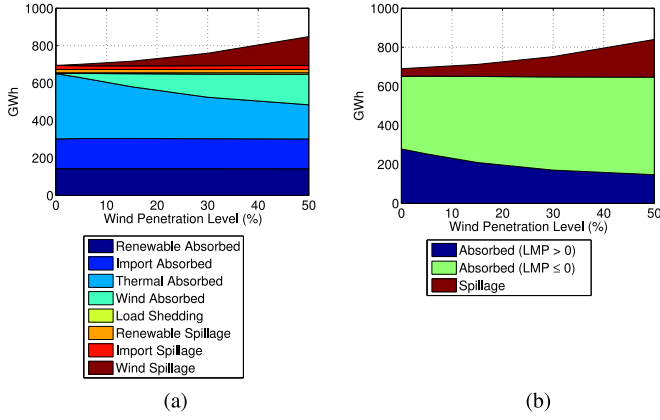
Fig. 6. Absorbed power, spillage, and total supply for increasing wind level (Case 1). (a) Absorbed Power. (b) Total Supply.
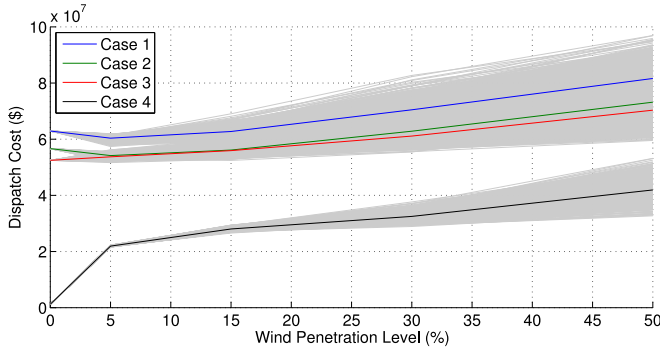

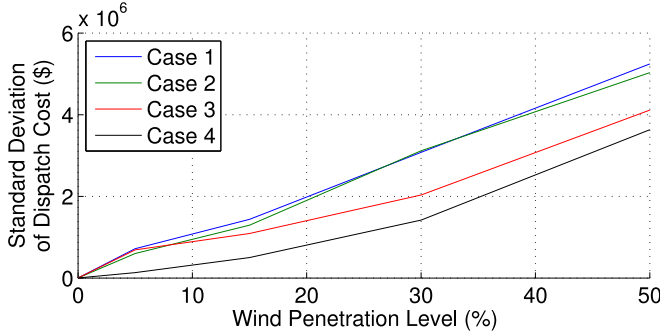Fig. 7. Dispatch cost at different wind levels.

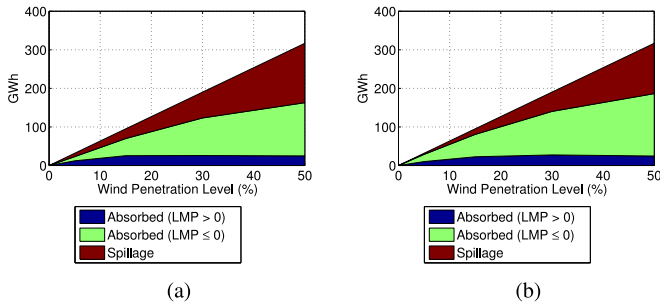Fig. 8. Standard deviation of dispatch costs at different wind levels.

Fig. 9. Wind supply by LMP and spillage. (a) Case 1. (b) Case 4.

TABLE II
THERMAL SUPPLY AND SPILLAGES AT DIFFERENT WIND LEVELS (GWH)

	Wind Level	RPS	Thermal Supply	Wind Spillage	Import Spillage	Renewable Spillage
Case 1	0%	22%	349	0	21	18
	5%	25%	325	8	19	18
	15%	32%	276	25	19	18
	30%	41%	221	66	20	18
	50%	47%	182	154	21	18
Case 2	0%	22%	439	0	14	18
	5%	25%	413	6	12	18
	15%	33%	361	19	12	18
	30%	43%	292	48	12	18
	50%	51%	238	122	13	18
Case 3	0%	22%	374	8	11	17
	5%	25%	355	17	11	17
	15%	32%	315	39	11	17
	30%	40%	272	86	11	17
	50%	45%	237	176	11	17
Case 4	0%	24%	358	0	0	0
	5%	28%	362	2	9	5
	15%	36%	309	14	11	7
	30%	45%	255	49	11	7
	50%	52%	220	130	11	8

To absorb the variability of the wind, total supply increases by 21% (from 689 to 839 GWh), even if there is increase in the load. At 50% wind penetration level, 23% of generation is spilled (*not absorbed* into the system). This result reflects the difficulty in achieving high RPS because of wind variability. Daily load shed for this case is also 8 GWh.

Fig. 6(b) shows daily average power by LMP value (price) and spillages. We recall that stranded power is the sum of spillage and power absorbed into the system at negative price (LMP≤ 0). We observe that as wind levels increase, both spillage and stranded power increase. Stranded power increases from 60% at a 0% wind level to 83% at a 50% wind level. While the total economic return for a generator may not be reflected in LMP alone, we note that the amount of power absorbed at positive price (profitable power) does not increase after a 15% wind level (see Fig. 9(b)).

B. Adding Data Centers

Fig. 7 compares dispatch costs for all cases. We note that the dispatch cost of the base system is decreased in all cases. The dispatch costs of the base system are decreased in Cases 2 and 3 by less than 5% at 0% wind level, respectively, and by less than 13% at a 50% wind level. These results indicate that adding data centers has a beneficial effect and that this value increases as more stranded power is present. Case 4 reduces the dispatch cost dramatically. A relative reduction of 98% is observed at 0% wind level and a relative reduction of 49% is observed at 50% wind level (compared with Case 1). As seen in Table II, the dramatic decrease in cost is due to minimization of spillage (penalized at large values). At a 0% wind level, in particular, dispatchable loads fully eliminate spillages. In Cases 2 and 3 we can see reductions in spillages, but these are much smaller than those observed in Case 4. In particular, we note

that optimally placed dispatchable loads (Case 4) favor spillage reductions of nonwind renewable supply over wind supply. This result supports the conclusion that dispatchable loads, when strategically placed, can provide much greater benefits for the power grid. The reason is that OP allows them to eliminate spillages from a variety of generators in types and locations and provides flexibility to manipulate network flows.

In Fig. 7 we observe that significant value is obtained in Case 4 at all wind levels, with benefits as great as 40% at the 50% wind level. At low wind penetration, the dispatchable loads eliminate essentially all spillage, dramatically reducing associated penalties. As the wind penetration level increases, the gap with respect to the base system is reduced. The decreased benefit is due to the large amounts of spillage that are introduced at high wind levels and that cannot be fully eliminated even with optimally located dispatchable loads. This situation is observed in Table II where wind power spillage increases proportionally to the wind level. Fully eliminating spillage would require additional data centers.

A surprising result is that the system cost variance is dramatically reduced with dispatchable loads. Fig. 8 illustrates this. In particular, the standard deviation for Case 4 is $0.1 MUSD/day at a 5% wind level and $3.6 MUSD/day at a 50% wind level. We recall that the standard deviations for Case 1 are $0.7 MUSD/day at a 5% wind level and $5.2 MUSD/day at a 50% wind level. For Case 2 the standard deviation is $0.6 and $5 MUSD/day at 5% wind level and 50% wind level, respectively. For Case 3 the standard deviation is $0.6 and $4.1 MUSD/day at 5% wind level and 50% wind level, respectively. For Case 4 we also note that variances are negligible for wind levels below 10% and remain small for wind levels below 20%. In contrast, the variances for Cases 1, 2, and 3 quickly increase with the wind level. The reduction in cost variance is the result of additional system spatiotemporal flexibility provided by dispatchable loads at different locations, which allows for network flow control.

C. Impact on Wind Generators

Of particular interest are the generation, spillage, and uneconomic and economic generation of wind power as the wind penetration level increases. Fig. 9 shows the growing wind supply, what fraction is spilled, and what fraction is absorbed in both uneconomic and economic terms. For brevity we show results only for Cases 1 and 4. Adding dispatchable loads decreases wind spillage significantly (to zero at low wind penetration and by more than 15% at high penetration). However, there is a complementary increase in the uneconomic power accepted by the grid, so the total stranded power remains large.

D. Data Center Achieved Capacity

Figs. 10(a) and (b) show the changes in the average achieved capacity during a day and the average increase in data center capacity achieved as wind level grows, respectively. We can see that a capacity of 20% is achieved at 0% wind level. This indicates that dispatchable loads are used to decrease spillages of nonwind renewables and imports but the data-center loads
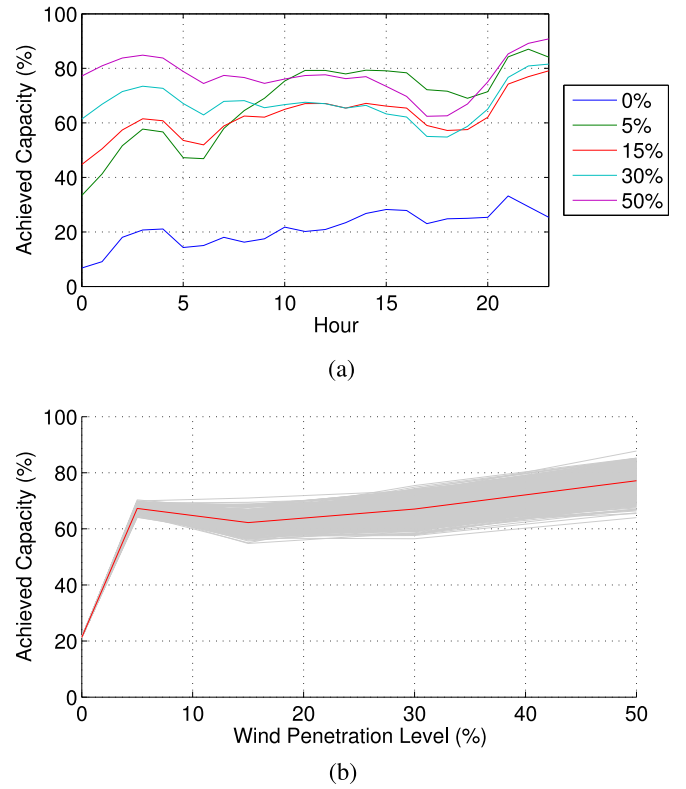

(a)

(b)

Fig. 10. Achieved fraction of data-center capacity in Case 4. (a) Average achieved capacity daily time profile at different wind penetration levels. (b) Total achieved capacity increase in wind level.

are far from fully served, an unattractive feature from a data-center owner standpoint. Achieved data-center capacity, however, increases rapidly to 60% at a 5% wind level (indicating that stranded wind power adds value to the loads). In addition, achieved capacity goes up to 80% at 50% wind penetration level, and the trend is maintained throughout the day. We found that the variance of the achieved capacity does not increase for wind levels higher than 15%. We also note that unserved loads for flexible data centers are not penalized in Case 4 (no demand elasticity price is provided) but high achieved data-center capacity can still be achieved. Consequently, we conclude that stranded power provides a natural economic incentive for flexible computing. In addition, the result indicates that the power grid indeed benefits from serving the data center loads.

V. SUMMARY AND FUTURE WORK

Our analysis shows that increased wind penetration levels lead to high levels of spillage and uneconomic absorbed generation, which together we call stranded power. Significant at even moderate levels of wind penetration, these numbers grow even higher at high levels of wind penetration (83% at 50% penetration). Two scenarios added data centers in conventional ways, alone and paired with a wind farm. However, a new kind of scenario, which optimally placed data centers as and treats them as dispatchable loads that the grid could turn on or off based on grid benefits, gave surprising results. Spillage and average power cost decreased dramatically; as much as 44%.

Dispatchable loads enable better utilization of wind generation and significantly more efficient and flexible network flow control, enabling dispatchable data center loads to achieve $60 \sim 80\%$ of full capacity. We highlight, however, that our conclusions are based on a particular case study that uses data published in the literature. Our work does not seek provide accurate estimates on performance (this would require using real system data and carefully crafted studies) but seeks to highlight the potential benefits of exploiting flexibility in loads at the scale provided by data centers. Our work also seeks to reveal non-intuitive limitations of placing data centers next to wind farms to harness local stranded power as opposed to optimally placing them to add network flexibility to harness stranded power throughout the system.

We highlight that, in this work, we assume fully flexible loads for the data center in order to understand what would be the potential economic opportunities from an ISO perspective and to understand what would be the best possible achievable served capacity. In future work we will model data center loads in more detail to identify impacts of load constraints. Such modeling would require detailed time-dependent data on typical job schedules and loads, which can vary greatly from data center to data center and thus need to be handled with care. Such models should also potentially incorporate scheduling logic for the data centers and will thus lead to significantly more computational complexity and will require of algorithmic advances.

REFERENCES

[1] Intergovernmental Panel on Climate Change, "Climate change 2014: Synthesis report," 2014. [Online]. Available: http://www.ipcc.ch
[2] A. Gore, "An inconvenient truth," *Documentary Film*, 2006.
[3] United Nations Framework Convention on Climate Change. (1997). *Kyoto protocol*. [Online]. Available: http://unfccc.int/kyoto_protocol/items/2830.php
[4] United Nations Framework Convention on Climate Change. (2015). *Paris climate change conference*. [Online]. Available: http://unfccc.int/meetings/paris_nov_2015/meeting/8926.php
[5] H. S. Dunn. (2010). *The carbon footprint of ICTS*. [Online]. Available: https://www.giswatch.org/thematic-report/sustainability-climate-change/carbon-footprint-icts
[6] Greenpeace. (2015, May). *Clicking clean: How companies are creating a green internet: 2015 update*. [Online]. Available: http://www.greenpeace.org/usa/wp-content/uploads/legacy/Global/usa/plan et3/PDFs/2015ClickingClean.pdf
[7] L. Barroso, *et al.*, *The Data Center as Computer: An Introduction to the Design of Warehouse-Scale Machines*. San Rafael, CA, USA: Morgan-Claypool, 2009.
[8] C. Patel *et al.*, "A cost model for planning, development, and operation of a data center," HP Labs, Palo Alto, CA, USA, Tech. Rep. HPL-2005-107R1, 2005.
[9] (2015). *Google makes its biggest renewable energy purchase yet*. [Online]. Available: http://www.datacenterknowledge.com/archives/2015/12/03/google-buys-842- mw-of-renewables-for-google-data-centers/
[10] (2014). *Apple to build a 3rd massive solar panel farm in North Carolina*. [Online]. Available: https://gigaom.com/2014/07/08/apple-to-build-a-3rd-massive-solar-panel-farm-in-north-carolina/
[11] Í. Goiri *et al.*, "Parasol and GreenSwitch: Managing datacenters powered by renewable energy," in *Proc. ACM SIGARCH Comput. Archit. News*, 2013, pp. 51–64.
[12] J. L. Berral *et al.*, "Building green cloud services at low cost," in *Proc. IEEE Int. Conf. Distrib. Comput. Syst.*, 2014, pp. 449–460.
[13] The Washington Post, "Use the Web? Congrats, you're an environmentalist," 2014. [Online]. Available: https://www.washingtonpost.com/news/wonk/wp/2014/11/06/like-kite-surfin g-the-internet-why-google-microsoft-and-yahoo-are-buying-up-wind-energy/
[14] X. Wang *et al.*, "Grid-aware placement of datacenters and wind farms," in *Proc. IEEE 6th Int. Green Comput. Conf. Sustain. Comput. Conf.*, 2015, pp. 1–8.
[15] I. Goiri *et al.*, "Intelligent placement of datacenters for internet services," in *Proc. 31st IEEE Int. Conf. Distrib. Comput. Syst.*, 2011, pp. 131–142.
[16] I. L. Zhenhua Liu, H. Mohsenian-Rad, and A. Wierman, "Opportunities and challenges for data center demand response," in *Proc. Int. Green Comput. Conf.*, 2014, pp. 1–10.
[17] N. Chen, X. Ren, S. Ren, and A. Wierman, "Greening multi-tenant data center demand response," *SIGMETRICS Perform. Eval. Rev.*, vol. 43, no. 2, pp. 36–38, Sep. 2015. [Online]. Available: http://doi.acm.org/10.1145/2825236.2825252
[18] Z. Liu, I. Liu, S. Low, and A. Wierman, "Pricing data center demand response," in *Proc. ACM Int. Conf. Meas. Model. Comput. Syst.*, 2014, pp. 111–123.
[19] A. A. Chien *et al.*, "The zero-carbon cloud: High-value, dispatchable demand for renewable power generators," *Electricity J.*, vol. 28, pp. 110–118, 2015.
[20] F. Yang *et al.*, "ZCCloud: Exploring wasted green power for high-performance computing," in *Proc. IEEE Int. Symp. Parallel Distrib. Process.*, May 2016, pp. 1051–1060.
[21] California Public Utilities Commission (CPUC). [Online]. Available: http://www.cpuc.ca.gov/PUC/energy/Renewables
[22] C. Megerian *et al.*, "Gov. Brown signs climate change bill to spur renewable energy, efficiency standards," *Los Angeles Times Newspaper*, Sep. 2015.
[23] Renewable energy 13.4% of US electricity generation in 2014. [Online]. Available: http://cleantechnica.com/2015/03/10/renewable-energy-13-4-of-us-electri city-generation-in-2014-exclusive/
[24] "Investigating a higher renewables portfolio standard in california: Executive summary," Report from Energy and Economics, Inc., Jan. 2014, [Online]. Available: http://ethree.com/
[25] D. Lew *et al.*, "Wind and solar curtailment," in *Proc. Int. Workshop Large-Scale Integration Wind Power Power Syst.*, 2013.
[26] O. A. Ben-Yehuda *et al.*, "Deconstructing Amazon EC2 Spot Instance pricing," *ACM Trans. Econ. Comput.*, vol. 1, no. 3, Sep. 2013, Art. no. 16.
[27] "Google compute engine: Creating a preemptible VM instance," [Online]. Available: https://cloud.google.com/compute/docs/instances/preemptible.
[28] W. Guo *et al.*, "Bidding for highly available services with low price in spot instance market," in *Proc. 24th Int. Symp. High-Perform. Parallel Distrib. Comput.*, 2015, pp. 191–202.
[29] V. M. Zavala *et al.*, "A stochastic electricity market clearing formulation with consistent pricing properties," Argonne Nat. Lab., Lemont, IL, USA, Tech. Rep. ANL/MCS-P5110-0314, 2015. [Online]. Available: http://arxiv.org/abs/1510.08335
[30] L. Yu, T. Jiang, Y. Cao, and Q. Zhang, "Risk-constrained operation for internet data centers in deregulated electricity markets," *IEEE Trans. Parallel Distrib. Syst.*, vol. 25, no. 5, pp. 1306–1316, May 2014.
[31] A. Papavasiliou and S. S. Oren, "Multiarea stochastic unit commitment for high wind penetration in a transmission constrained network," *Oper. Res.*, vol. 61, no. 3, pp. 578–592, 2013.
[32] M. Bastian *et al.*, "Gephi: An open source software for exploring and manipulating networks," in *Proc. 3rd Int. AAAI Conf. Weblogs Social Media*, 2009, vol. 8, pp. 361–362.
[33] M. Lubin *et al.*, "Computing in operations research using Julia," *INFORMS J. Comput.*, vol. 27, no. 2, pp. 238–248, 2015.
[34] J. Huchette *et al.*, "Parallel algebraic modeling for stochastic optimization," in *Proc. 1st First Workshop High Perform. Tech. Comput. Dynamic Lang.*, 2014, pp. 29–35.
[35] K. Kim *et al.*, "Algorithmic innovations and software for the dual decomposition method applied to stochastic mixed-integer programs," *Optim. Online*, 2015.

[36] M. Wilde, M. Hategan, J. M. Wozniak, B. Clifford, D. S. Katz, and I. Foster, "Swift: A language for distributed parallel scripting," *Parallel Comput.*, vol. 37, no. 9, pp. 633–652, 2011.
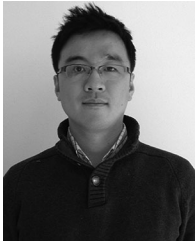
Kibaek Kim received the B.S. degree from Inha University in Korea, Incheon, South Korea, the M.S. and Ph.D. degrees from Northwestern University, Evanston, IL, USA, all in industrial engineering. He is a Postdoctoral Appointee in the Mathematics and Computer Science Division, Argonne National Laboratory, Lemont, IL, USA, since 2014. He currently serves as a Reviewer in several peer-reviewed journals, including *Operations Research*, *Computational Optimization and Applications*, *European Journal of Operational Research*, and *IIE Transactions*. He is a main developer of DSP, the parallel stochastic mixed-integer programming solver used for the computational studies in this paper. His research interests include modeling and parallel algorithms for large-scale optimization problems in application to network design, planning, and operations.
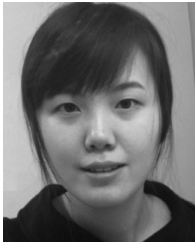
Fan Yang received the B.Eng. degree in computer science from the National University of Defense Technology, Changsha, China, in 2012. She is currently working toward the Ph.D. degree in the Department of Computer Science, University of Chicago, Chicago, IL, USA. She joined the Large-Scale System Group, University of Chicago, in 2013. She has broad research interests in parallel and distributed systems, data-intensive computing, parallel programming and optimization, large-scale system software, and computer architecture. In the past year, she worked on graph computing and benchmarking of graph-processing systems. She currently focuses on green datacenter design and stranded power in renewable electricity generation.

Victor M. Zavala received the B.Sc. degree from Universidad Iberoamericana, Mexico City, Mexico, and the Ph.D. degree from Carnegie Mellon University, Pittsburgh, PA, USA, both in chemical engineering. He is the Richard H. Soit Assistant Professor in the Department of Chemical and Biological Engineering, University of Wisonsin-Madison, Madison, WI, USA. Before joining UW-Madison, he was a Computational Mathematician in the Mathematics and Computer Science Division, Argonne National Laboratory. He received the Department of Energy Early Career Award under which he develops scalable optimization algorithms for infrastructure networks. He is also a Technical Editor of *Mathematical Programming Computation*. His research interests include the areas of mathematical modeling of energy systems, high-performance computing, stochastic optimization, and predictive control.

Andrew A. Chien received the B.S., M.S., and Ph.D. degrees at the Massachusetts Institute of Technology, Cambridge, MA, USA. He is the William Eckhardt Professor in computer science at the University of Chicago, the Director of the CERES Center for Unstoppable Computing, and a Senior Computer Scientist at Argonne National Laboratory. His research interests include parallel computing, computer architecture, and cloud computing. His research has been recognized with an NSF Young Investigator Award, and numerous best paper awards. He serves as Cochair of the CACM editorial board. From 2005 to 2010, Chien was the Vice President of Research at Intel, launching initiatives in parallel software, mobile computing, cloud computing, and and exascale research. From 1998 to 2005, he was the SAIC Professor where he founded the Center for Networked Systems, UCSD. From 1990 to 1998, he was a Professor at the University of Illinois and NCSA. He has served on numerous advisory committees for the NSF, DOE and universities such as Stanford, EPFL, UW, and Cal-Berkeley. He is a Fellow of the ACM and AAAS.